CFD investigation of fluid flow within elbow pipes

Anshika Trivedi, *Rajneesh Kumar, Aditya Veer Gautam*
Email Id: - anshikatrivedi9455@gmail.com
Department of Mechanical Engineering, Faculty of Engineering& Technology, Rama University, Kanpur (U.P). India

Abstract: Elbow pipes are crucial parts of many fluid transport systems, including ones used in the oil and gas industry. The curved shape of such pipes induces centrifugal forces on the internal flow, ultimately affecting the flow velocity and creating pressure differences within the elbow.

The present study is an investigation of the effects of elbow pipes on the flow, and how changing the curvature ratio of an elbow pipe affects the internal flow. The study entails three-dimensional numerical simulations and analysis for laminar internal flows within pipes of varying curvature ratios. For laminar flows, the simulations are based in 4 Reynolds numbers ranging from 200 to 2000 and 3 curvature ratios R_o = 2.8, 5.6 and 11.2. A mesh convergence study is carried out for 3 meshes of increasing resolution. The optimal mesh is then compared to published experimental and numerical results for validation. Once the validation is confirmed, further simulation and analysis is performed for each combination of curvature ratio and Reynolds number. The results reveal that the flow separates due to the centrifugal forces induced by the curved shape. They also show that secondary flows consisting of symmetrical helical vortices called Dean Vortices are generated. The intensity of this secondary flow is shown to increase as the Dean number increases.

Keywords: Curved pipe, elbow, laminar flow, Dean Vortices, CFD, Open FOAM.

1. INTRODUCTION

The present study conducts a numerical investigation of three-dimensional (3-D) laminar internal flow within a 90-degree elbow pipe. A baseline elbow pipe geometry is created to be used for numerical simulations. The pipe consists of an inlet part of 50D length, an outlet part of 20D length and a pipe bend with curvature ratio $Ro=Rc/Rp$, where D is the diameter of the pipe, Rp is the radius of the pipe $D/2$, and Rc is the pipe curvature . This curvature ratio is modified for each case study. The main purpose of this study is to investigate how changing the curvature ratio, R_o, and the Re affects the elbow internal flow. Firstly, the results of the present numerical study are validated by comparing it to previously published experimental and numerical results. Once the validity of the study is confirmed, the further study is carried out.

Four different Reynolds numbers ranging from 200 to 2000 and three different curvature ratios for each Reynolds number adopted for the simulation. Numerical simulations for the purposes of this study are carried out using the Gorina cluster, a supercomputer at University of Stavanger.

Background:

In multiple engineering applications, such as the oil and gas industry, fluid transport is an essential part of the process. The extracted oil and gas are transported by pipelines from the subsea reservoirs to topside. After the fluid is extracted it travels within a series of pipes which are fitted together by different pipe fitting types, namely elbow, tee, and Y-junctions. Due to the different geometries of the pipes, they are subjected to pressure and velocity variations within the internal flow. This results in high-pressure regions in the flow which create a higher load on the pipe wall, and low-pressure regions, which allow the outer pressure to have a greater effect on the pipe wall. These are factors that must be taken into consideration in the design process of

such fittings and pipes. With the ever-increasing demand for energy, any method that improves planning prior to well operation will improve the economic feasibility and allow for operation in more parts of the world.

As high-speed computer technology continues to evolve, so does the capability of computational fluid dynamics (CFD). CFD analysis is a powerful and cost-effective way of studying fluid flow problems. This is particularly useful in many aspects of the offshore petroleum industry, such as design of oil and gas separators, drill bits and pipelines to mention
a few. Creating an accurate representation of the real-life flow allows for prediction of the fluid flow. The prediction of the flow can be used as a verification of the product, before putting it into production, thus reducing the costs of testing and overall development. It allows for optimization of products and processes by avoiding excessive costs. Running CFD simulations is not time consuming and allows gathering of engineering data in the early phases of the design process, compared to more time-consuming experiments. The data gathered is valid for the whole specified flow domain, while physical testing limits the amount of data gathered to areas where sensors and gauges are placed. This makes CFD analysis very flexible, as the designer may investigate any region of interest in the flow domain and can easily change the model to simulate different conditions. It is essential to find a model that accurately represents the flow, but also does not use unnecessary processing power. This optimalization can be found through convergence study, where multiple meshes of increasing density are compared to check for convergence of the simulations. This way, the mesh with lowest grid resolutions can be checked with a higher grid resolution to determine if it can provide satisfactory results.

Published work

Many studies focusing on flow within pipes and, specifically, elbow pipes, have been conducted. This section will briefly present some of the most relevant numerical and experimental studies that have previously been performed.

An experimental study was performed by Sudo et al. (1997). The study included experiments of turbulent flow in a 90-degree bent pipe. The curvature ratio of the elbow was $Rc/D=2$ and the pipe had a diameter of $D=104\ mm$. An inlet pipe of 100D was connected to the elbow, allowing the flow to be fully developed. Measurements were taken for air entering the pipe with mean velocity of 8.7 m/s, corresponding to a Reynolds number of $Re = 60000$. This value was used as the reference to previous work conducted by Enayet et al. (1982) and Azzola et al. (1986). Nicolaou and Zaki (2016) numerically investigated both laminar and turbulent flows within curved pipes. Pipe simulations were mainly used to represent the flow in the upper breathing airways. Their investigation included pipe simulations for Reynolds numbers of $Re=1000$ for the laminar case and $Re=10000$ for the turbulent case.

was created with diameter D=0.01 m, inlet length D, outlet length $2D$ and curvature radius Rc=2.8D. The finite volume formulation presented by Rosenfeld, Kwak and Vinokur (1991) were used in the numerical simulations. Another numerical investigation of laminar flows within elbow pipes was conducted by Inthavong (2018) for the purposes of studying particle deposition in human airways. 8 diameters ranging from 0.005 to 0.100 m, 9 bend radii ranging from 0.006 m to 0.070 m and 3 different Reynolds numbers, 400, 1000 and 2000 were investigated in this study. A template geometry was created consisting of a straight inlet pipe of 5D, a straight outlet pipe of 3D and an elbow with curvature ratio 5.6. Numerical simulations were carried out for 48 combinations of diameters, curvature ratios and Reynolds numbers.

Theory

The present chapter, the theory of internal pipe flow of viscous fluids is explained in detail:-

Laminar and turbulent flows

In general, flow regimes can be laminar or turbulent. A laminar flow is characterised by highly ordered and smooth flow. On the contrary, turbulent flow is chaotic with pressure and velocity changes occurring throughout the flow. These flow motions can be visualized by injecting a dye into the flow. The dye injected into laminar flow will produce a linear streamline, while the turbulent flow will produce a disordered streamline. The concept of laminar and turbulent flows was first demonstrated by Osborne Reynolds in 1884.
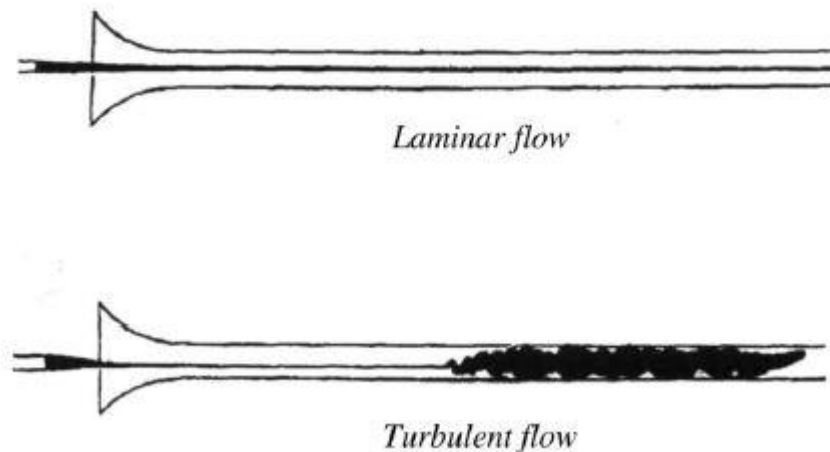

Figure 1 Notes from Osborne Reynolds' flow experiment

Figure 1 illustrates how the injected dye in laminar flow stays ordered and constant through the entire region. In the turbulent flow region, the dye gets mixed due to the highly disordered nature of the flow.\

Reynolds number

The Reynolds number is a dimensionless parameter which is used to classify the type of flow that occurs in a pipeline. The Reynolds number is given by

$$Re = \frac{inertial\ forces}{viscous\ forces} = U_{avg}D/\nu$$

where $Uavg$ is the average velocity of the flow$D$ is the characteristic length of the pipe, and $v=(\mu/\rho)$ is the kinematic viscosity of the fluid. It is observed that low viscosity fluids, flowing at high velocity have high Reynolds number. According to Çengel & Cimbala (2017), laminar flow is characterised by $Re\leq2300$. For turbulent flows, $Re\geq4000$. Flows where $2300\leq Re\leq4000$ are called transitional flows. These are flows that contain regions of both turbulent and laminar flow.

Entrance region

At the inlet of a pipe, the velocity flow field is uniform in the direction of the flow. At this point, the particles of the fluid that are in contact with the pipe wall are stopped due to the no-slip condition. Connecting layers are affected by this friction causing a gradual velocity decrease from the midsection of the pipe to the walls. To compensate for this velocity reduction, the velocity must increase at the pipe midsection to conserve the mass flow rate. As the flow progresses through what is called the hydrodynamic entrance region, the viscous forces of the fluid start affecting the flow field. The flow is divided into two main regions, an irrotational flow field, where the viscous forces are negligible and velocity remains constant, and a flow field where viscous forces slow down the fluid. The flow field will continue to develop as it gets further into the pipe, until it is fully developed. The region where the flow is fully developed is called the hydrodynamic fully developed region.
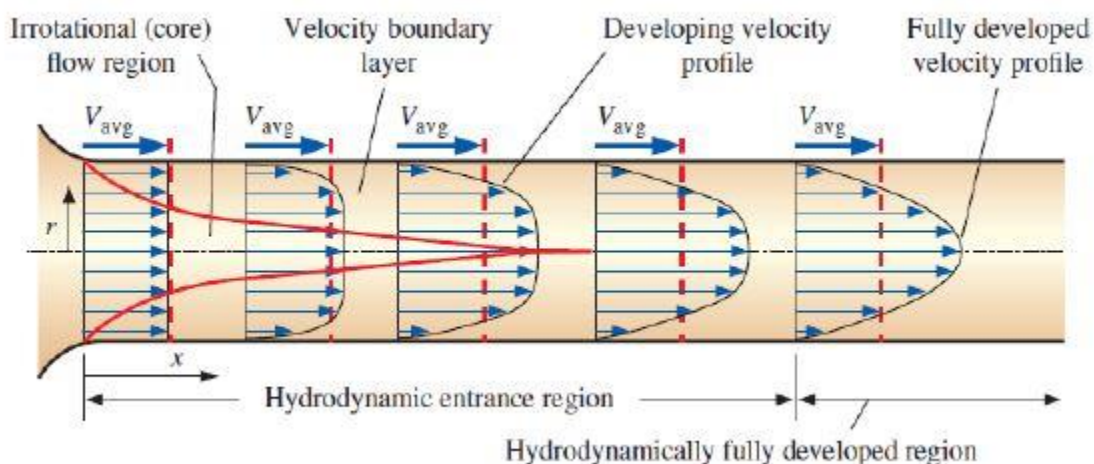

Figure 2 Development of the velocity profile of internal fluid flow (Çengel & Cimbala, 2017, p.355)

The shape of the fully developed velocity profile differs between laminar flow and turbulent flow. Figure 2 exhibits a fully developed laminar flow. The velocity field is characterised by a parabolic shape. A fully developed turbulent flow is characterised by a significantly flatter 6

shape than that of the laminar flow field. This is due to the eddy motions, and more prominent mixing in the radial direction.
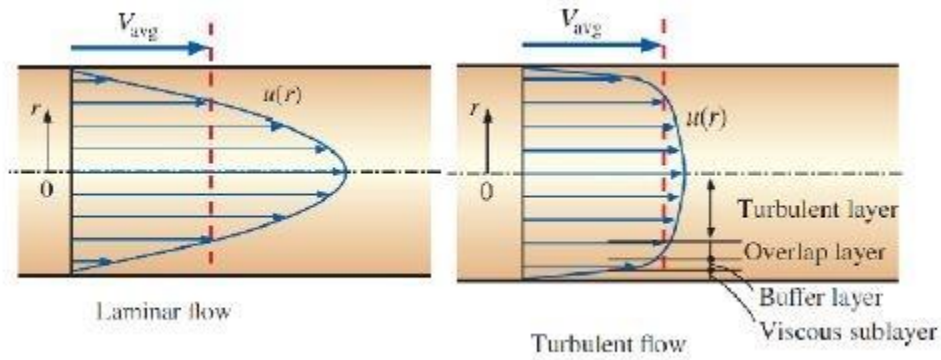
Figure 3 Fully developed laminar (left) and turbulent (right) flows (Çengel & Cimbala, 2017 p.368)

Entrance length

The length of the entrance region for laminar flows is defined as the distance from the inlet to where the wall shear stress is within about 2% of the fully developed value. The entrance length for laminar flow is given by L

$$laminar \cong 0.05 Re \times D$$

For $Re = 200$, the resulting entrance length is $10D$, meaning that at $10D$ from the inlet the flow field will be close to fully developed.

In turbulent flow, however, the entrance length is much less dependent on the Reynolds number, resulting in a significantly shorter entrance region compared to high Reynolds number laminar flow. Entrance length for turbulent flow is given by

$$L_{turbulent} \cong 1.359 Re^{14} \times D$$

Generally, the entrance length in turbulent flow can be approximated to $10D$ for most practical engineering purposes, as the effects of the entrance region are insignificant beyond this point.
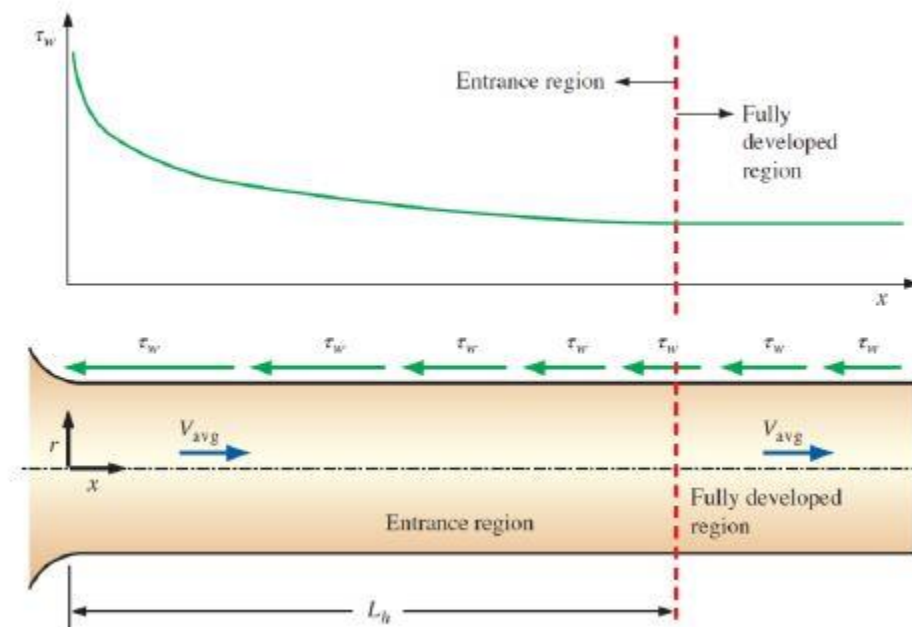
4578

Figure 4 The shear wall shear stress decreases gradually as the flow develops from the entrance region to the fully developed region (Çengel & Cimbala, 2017 p. 356)

Flow within curved pipe

As the fully developed laminar flow enters a curved pipe, it will get affected by the centrifugal forces of such a curved path. Dean (1928) investigated flow within curved pipes and showed that the faster moving central core of the fluid would be forced towards the outer curve of the pipe from the center. This effect is caused by the centrifugal force. However, the fluid closer to the inner wall moved towards the lower pressure region closer to the bend curvature center. In the circular cross-section of the pipe, a secondary flow consisting of two counter-rotating helical vortices occurred radial to the flow direction. These vortices are also known as Dean vortices

The Dean number is a dimensionless ratio, providing information about the effects of viscous forces to the centrifugal force within the curved pipe. It is given by

$$De=(RpRc)0.5$$

Where Re is the Reynolds number, Rp is the radius of the circular pipe cross section and Rc is the radius of the pipe curve. The value of the dean number says something about the occurrence of the previously mentioned vortices. *For De* $< 40\text{\textasciitilde}60$, the flow is completely unidirectional. At $De < 60\text{\textasciitilde}75$ small, wavy perturbations may be observed, implying the occurrence of a secondary flow. As the Dean number increases beyond this value, these wavy perturbations become increasingly significant, and the secondary flow gets more pronounced.
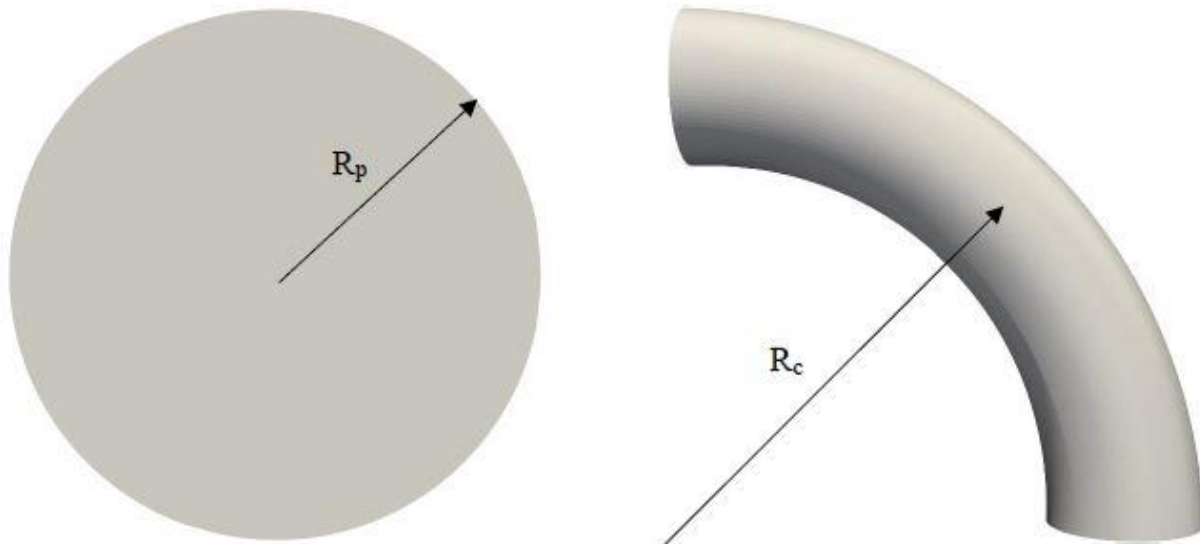
Figure 5 Rp and Rc used in the calculation of the Dean number

Computational Modelling

The principles of Computational Fluid Dynamics are briefly explained in the present chapter. An introduction to the open source CFD software OpenFOAM is also included as well as mesh theory

Computational fluid dynamics

CFD is a branch of fluid mechanics that applies numerical methods and modelling to predict fluid flow. It is a powerful tool for predicting and solving fluid flow problems. Fluid flow is modelled by sets of governing equations. These equations have proven to be difficult to solve analytically, and thus computational technology has been applied to optimize the process. The process of defining and solving a CFD problem can be divided into three main parts:

(i) Pre-processing

The first step of setting up the CFD problem is called the pre-processing stage. In this step, a geometry of the problem at hand is first created. A fluid flow domain is defined and constricted by boundary conditions. The created geometry is then divided into many smaller elements which make up the mesh. Mesh generation is carried out in software such as ANSYS, Pointwise, SALOME, GMSH and more.

(ii) Solving

Depending on the problem at hand, an appropriate solver is selected. Parameters such as initial conditions, turbulence model and solvers are defined in this stage. These solvers are implemented in the many available CFD software

(iii) Post-processing

In the final stage of the simulation process, the results obtained from the previous stage are processed in order to better visualize the problem. Data are extracted and used to plot velocity profiles, pressures and to create contour plots.

Analysis procedure
In CFD analysis, a step-by-step procedure is carried out for solving the conservation and transport equations. The procedure contains 8 steps (Çengel & Cimbala, 2017). The first stepis to create a computational flow domain and mesh. This is done through CAD software. In the case of this project, the domain is three-dimensional (3-D). The mesh is comprised of smaller volumes called cells. Discretized versions of the governing equations are to be solved for each cell. In this step, a high grid quality must be assured, thus assuring a high-quality solution. Once the mesh has been generated, boundary conditions should be applied on the surfaces of the geometry. For a pipe, this includes the inlet, outlet, and pipe wall. The third step is to specify fluid properties. This depends on the type of fluid and the flow conditions. Usually, properties such as density and viscosity are specified.

In this step numerical parameters for solving and a solving algorithm should be selected. These vary depending on the type of software that is used. An appropriate solver must be selected for the problem at hand. There are different appropriate solvers depending on flow properties, such as the compressibility and if the flow is steady or unsteady. Numerical parameters such as time steps and number of utilized processors in case of parallel simulation are determined.
The solution is calculated through an iteration process. A starting point must therefore be specified. These are the initial conditions. Parameters such as velocity and pressure at the start of simulation are quantified in this step.

Once the previous steps have been completed, solving of the discretized governing equations can begin. As previously mentioned, the solution process is iterative, meaning that the governing equations are solved iteratively at the centre of each cell, for each time step of the simulation. The result of putting all the terms of the Navier-Stokes equation to one side of the equation and summing them together, is called the residual. The residual should be zero for each cell. However, this is not the case for a CFD solution, but as the simulation progresses and more iterations are calculated, the residual will hopefully be effectively zero. Residuals are a measure of deviation from an exact solution. The smaller the residual, the more accurate the results are.

After the simulation is complete, and solutions have converged, the results may be post-processed. This entails plotting and graphical analysis of pressure and velocity. Contour plots are great visualizations of the pressure and velocity variations in the flow.

OpenFOAM

OpenFOAM is one of many available CFD software. It is short for Open Field Operation And Manipulation. The software is primarily used to solve fluid dynamics problems. The capabilities of the software are applicable in solid mechanics problems as well. OpenFOAM employs finite volume analysis to solve problems. This involves numerical solving of partial differential equations within the cell volumes that make up a mesh.

Operation of OpenFOAM follows a specified structure within a case directory folder. Any case must contain the three subfolders "0", "constant" and "system"

"0": This folder contains scripts that define the initial conditions of parameters such as pressure and velocity. Boundary conditions are also defined for these variables.

"constant": Within this folder, information about the physical properties of the case and the mesh is found. "system": The scripts within this folder define the settings for the simulation itself. This includes numerical schemes and solver methods.

Mesh quality

In CFD, the continuity and transport equations are solved for smaller subdomains. These subdomains are called cells and they build up the mesh. The accuracy of the solution is dependent on the quality of the mesh. There are multiple factors that determine the quality of the mesh, such as mesh types, skewness of cells, and cell density. In this section, these factors are explained.

Mesh types
Mesh types can be divided into primarily two groups: unstructured and structured meshes. Unstructured meshes are characterized by the arbitrary arrangement of cells. The shape of the cells varies throughout the mesh. A structured mesh, however, consists of neatly arranged cells. The cells may be distorted but follow a strict numbering system using indices.
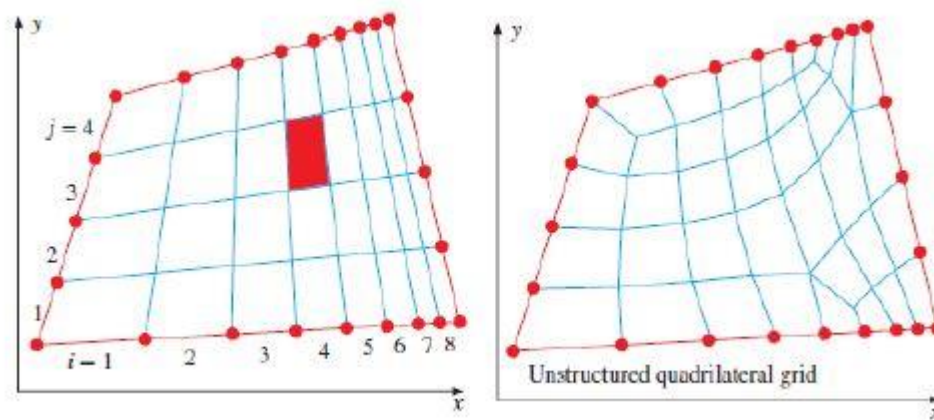

Figure 6 A structured (left) and an unstructured (right) quadrilateral mesh (Çengel & Cimbala, 2017, p. 890)

Complex geometries may require the use of a combination of the two. Hybrid meshes include regions where the mesh is structured, and other regions where unstructured meshes are more appropriate.

Depending on the dimension of the flow domain, different cell types are applied. For 2-D flow domains the cells are surfaces, and for 3-D flow domains, the cells are volumes. For hybrid meshes, different cell types may be applied where they are most appropriate. 2-D hybrid meshes may utilize both triangular and quadrilateral cells.
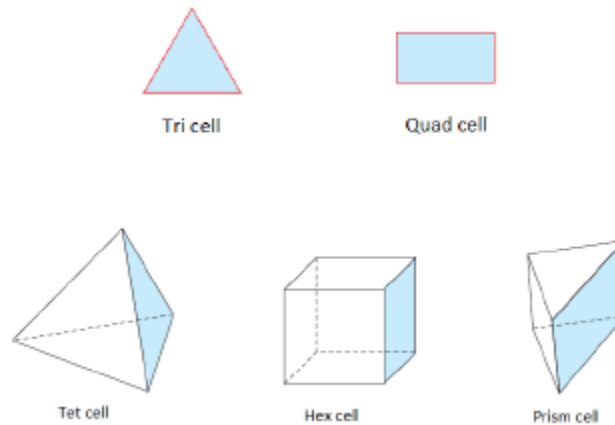
4582

Figure 7 Mesh cell types. The top row shows 2-D cell types, while the bottom row shows some 3-D cell types (Çengel & Cimbala, 2017, p. 894)

Numerical set-up

This chapter explains the numerical set-up of the study in detail, from geometry and mesh creation to case folders in OpenFOAM.

In order to produce a mesh, a geometry must be created. A geometry is created as the basis of the multiple cases that are to be compared. The geometry at hand is a cylindrical pipe with a 90-degree bend. Gmsh is the software used for the purposes of both geometry creation and mesh generation.

Firstly, the Geometry is created through a series of point and line creations. The geometric properties of the elbow pipe are given in the following table.

The effects of increasing the curvature ratio will be further studied. Other geometrical properties such as inlet and outlet length are kept the same for each case. Figure 8 shows the geometry used as a baseline for geometry and mesh creation of subsequent cases
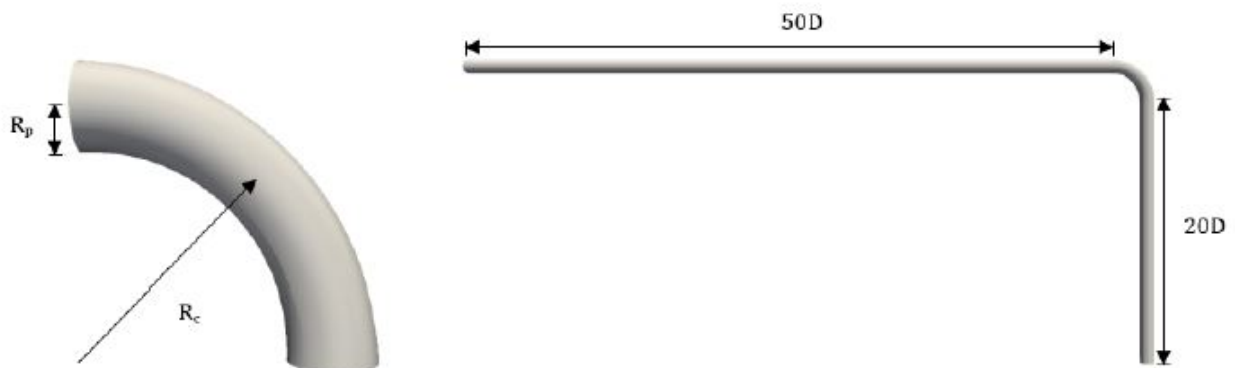

Figure 8 Geometrical model of elbow pipe baseline

4583

With lines created, the surfaces and volumes can be defined. Once surfaces are defined, the physical boundaries can be selected where the boundary conditions of the simulations will be set. The inlet and outlet are also specified as boundaries.

Mesh generation

Transfinite lines are defined for mesh generation. These parameters will determine how many mesh elements are generated. To reduce simulation time and capture large gradients of the flow variables at some regions, such as the near-wall regions and the bend pipe part, grid stretching will be applied. This means that the straight parts of the pipe will be coarse relative to the bent part of the pipe. The bent part will be the focus for accurate analysis and will therefore have a finer mesh. Once the geometry is finalised, gmsh can generate a mesh. For the first case the baseline mesh contains 1413733 elements. The number of mesh cells for each case is given.
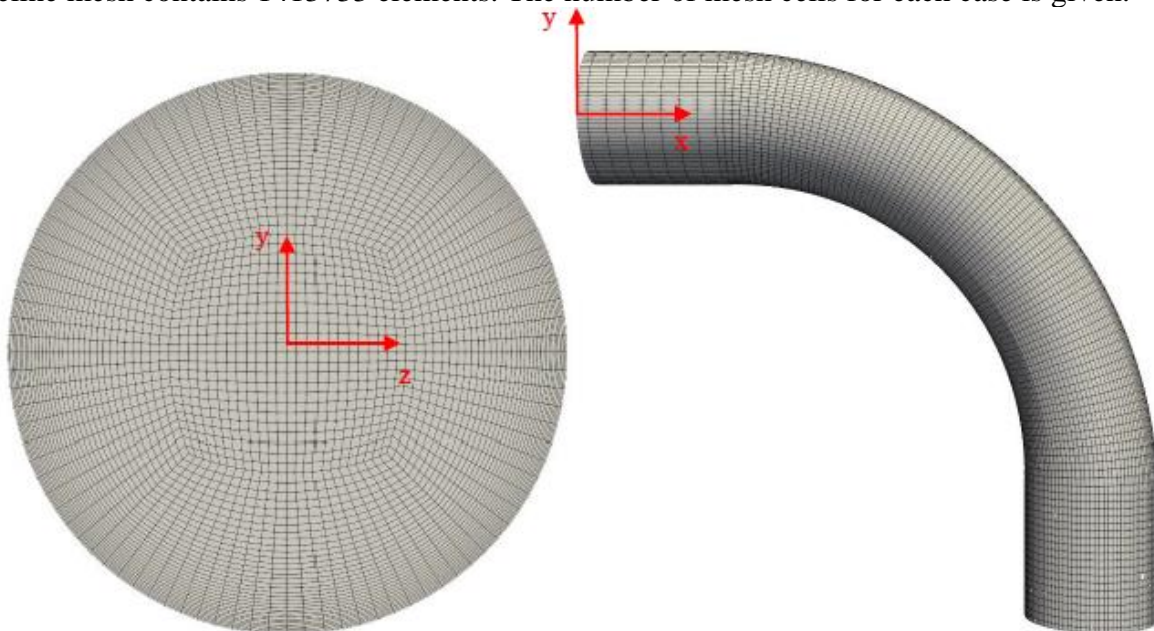

Figure 9 Cross section and profile of mesh 1

Figure 9 exhibits the mesh for Case 1. It clearly shows the relatively coarse mesh of the straight parts of the pipe, compared to the finer mesh of the pipe bend. The mesh resolution also gets finer closer to the pipe wall, as seen in figure 4-2. The reason for this is to account for the no-slip condition near boundary walls.

Laminar flow within elbow pipe

In this chapter, a detailed explanation of the numerical investigation of flow within elbow pipes of varying curvature ratio and Reynolds number is presented. A grid convergence and validation study are conducted for three different mesh sizes. This entails a comparison of the mesh sizes to check for grid independence, and comparison with published results to select the optimal mesh. The effects of varying Reynolds numbers and curvature ratios on the velocity profiles are explored, and the results of the simulations are illustrated in plots.

Pre-processing

As explained in chapter 3, the pre-processing step starts with geometry creation and grid generation. Three different geometries are created. The inlet and outlet lengths and pipe diameter remain the same for each geometry. The only variable, geometry-wise, is the curvature ratio, Rc. The curvature ratio is defined as

$$Ro=RcRp$$

where Rc is the radius of the curve and Rp is the radius of the pipe. The values of the curvature ratios investigated in this study are $Ro=5.6,11.2,22.4$. These values have been selected based on the studies conducted by Nicolaou and Zaki (2016) and Inthavong (2019), who investigated similar curvature ratios.
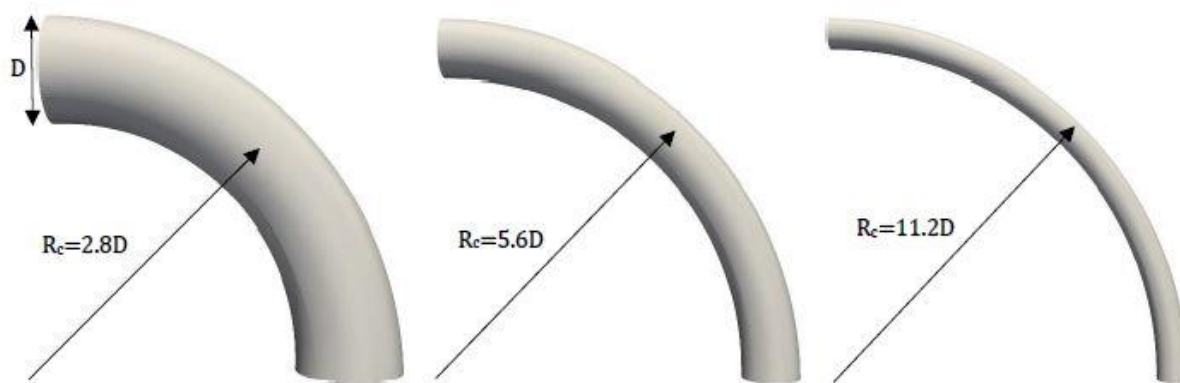

Figure 10 Geometry of elbows with bend radii $Rc=2.8D,5.6D,11.2D$, corresponding to curvature ratios of $Ro= 5.6,11.2,22.4$ (left to right)
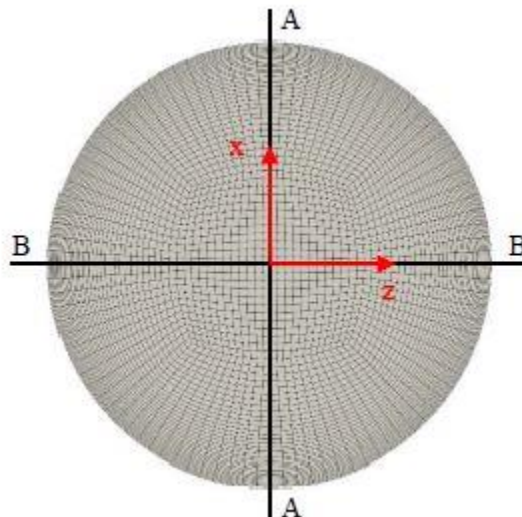

Figure 11 Cross section of pipe illustrating the diameters along which the velocity profiles have been plotted

The elbows all have a cross-sectional diameter of $D=0.01$. An inlet pipe of length $50D$ and an outlet pipe of $20D$ are connected to each elbow as well. The boundary conditions are defined at the inlet, pipe wall and outlet.

4585

Inlet: In the streamwise direction, a parabolic velocity profile enters the flow domain. It is given as $ux=2ua[(1-rR)2]$ with $uavg=1$ m/s and $uy=uz=0$. Pressure at this boundary is defined as zero normal gradient.
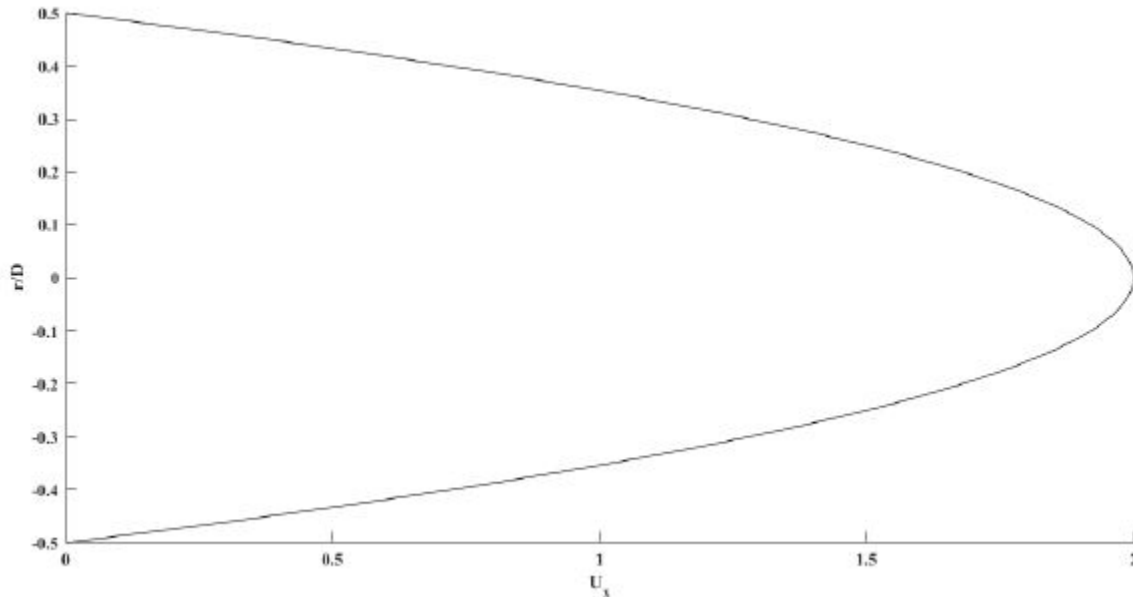

Figure 12 Velocity profile of laminar flow within the inlet pipe

Wall: The no-slip condition implies that the velocities at the wall are all zero. The pressure is set as zero normal gradient.

Outlet: Velocity is set as zero normal gradient and pressure is set to be zero

Steady state simulation

The case is ready for simulation once the mesh has been generated and the initial and boundary conditions have been set as well as simulation control parameters. Since a steady simulation is carried out, an important step after the simulation has been completed is to ensure that the simulation has reached a steady state. This is done by detecting the pressure value at each iteration step inside the elbow by using a probe. The probe location is defined in the 'controlDict' script in the 'system' folder and is set to be at the middle of the elbow itself prior to the simulation and is used to measure the pressure. The simulation outputs a text file containing the pressure value at the probe location at each iteration of the simulation.
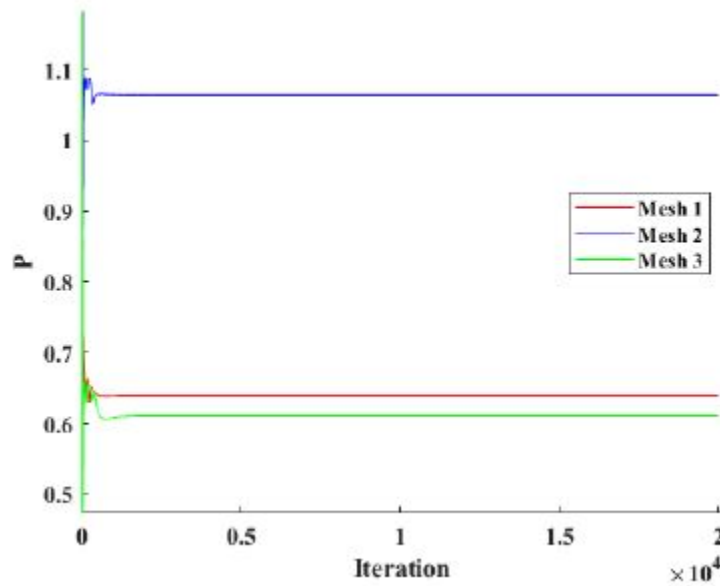
Figure 13 Pressure at the probe for three different mesh resolutions

illustrates the steadiness of three simulations: one for each mesh resolution. Large fluctuations can be observed at the very beginning of the simulations. The fluctuations quickly become a straight line, which is characteristic for a steady state simulation of laminar flow. From these results, it is concluded that the simulations of these mesh resolutions have reached a steady state.
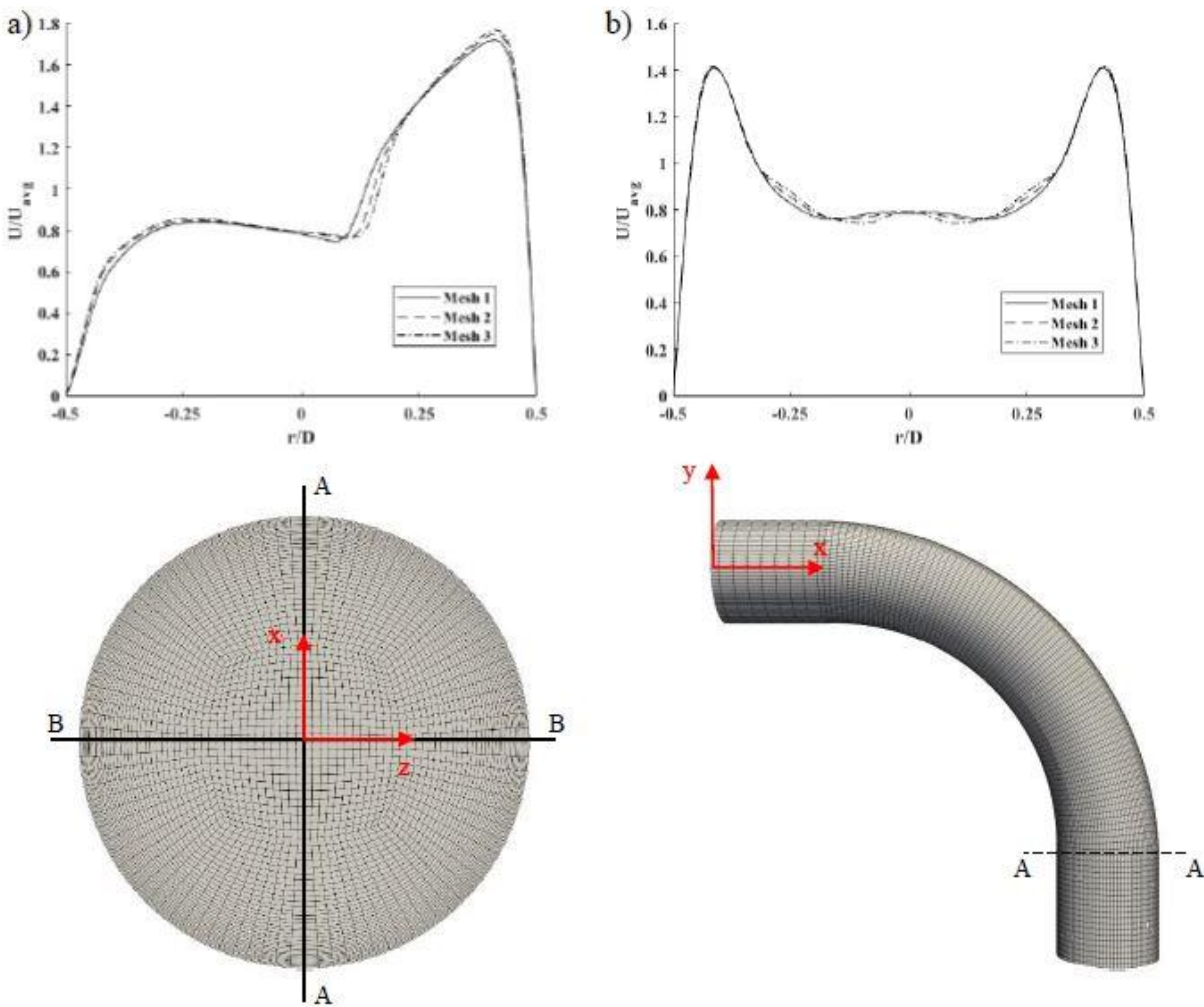
Figure 14 Convergence study of three different mesh sizes. a) illustrates the velocity profile along the A-A diameter and b) the velocity profile along the B-B diameter in the streamwise direction

Figure shows the velocity profiles at specified diameters located at the bend outlet. The left plot corresponds to the velocity profile at 90o of the bend parallel to the symmetry plane (A-A diameter), while the right plot shows the profile at the diameter perpendicular to the symmetry plane (B-B diameter). The graphs exhibit areas where the different mesh resolutions clearly deviate from each other. Mesh 1 deviates from mesh 2 and 3, however, the deviation between mesh 2 and 3 is relatively smaller, comparatively. As this is the case, the decision was made to proceed with validation using the mesh resolution of mesh 2. Once the convergence study is complete, the results obtained using the optimal mesh are validated against the experimental data or other published numerical results. This involves a comparison of results from the present study, to the results of previously published experimental and numerical results. For validation purposes, the velocity profiles at the A-A and B-B diameters are compared to the findings of Nicolaou and Zaki (2016).
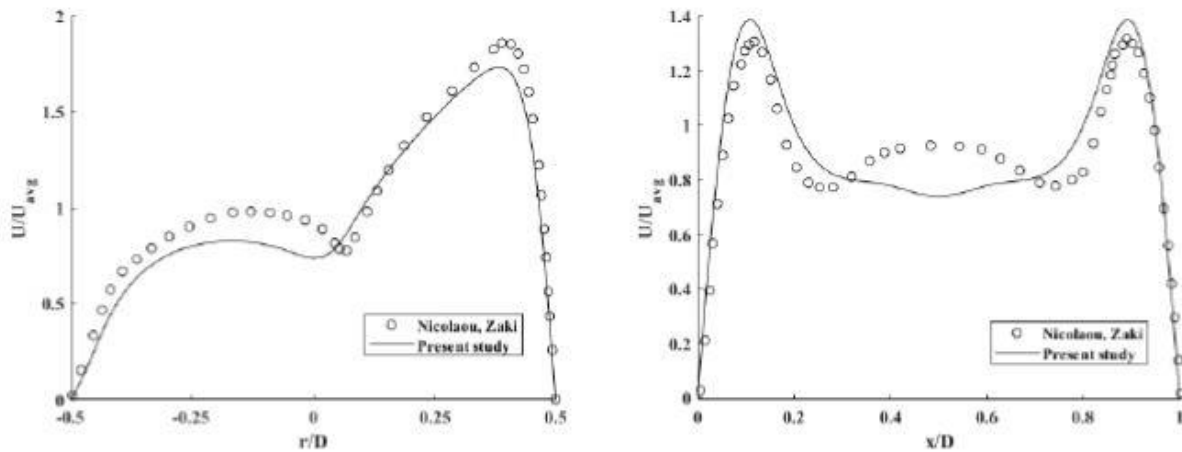
Figure 15 Validation study comparing mesh 2 with the findings of Nicolaou and Zaki (2016)

The results shown in figure 5-6 are for Re=1000, Ro=5.6 and D=0.01 m using the grid resolution of Mesh 2, in accordance with the values used in the reference study. The shape of the profile shows relatively good correspondence with the previously published results. There is some significant deviation in certain areas of the pipe, which may have occurred due to the usage of a longer inlet pipe than the one used in the study of Nicolaou and Zaki (2016). The peak values of the profile near the pipe wall have been captured well.

Results and discussion

In this section, the post-processed results from the simulations of the laminar flow inside the elbow pipes are presented. 12 simulations were carried out for all combinations of Reynolds numbers and curvature ratios. The values of Reynolds numbers used in the present study are Re=200,500,1000 and 2000. The curvature ratios Ro=5.6,11.2,22.4 are subjected to flows at each of the Reynolds number values. The post-processing software Paraview has been used to visualize the results of the simulations. Velocity contour plots have been created to illustrate the behavior of the fluid. The velocity contour plots shown in figure 15 show the velocity magnitudes at a cross section of the symmetry plane, accompanied by circular cross sections at the 90-degree outlet of the elbow. The circular cross section velocity contour plots
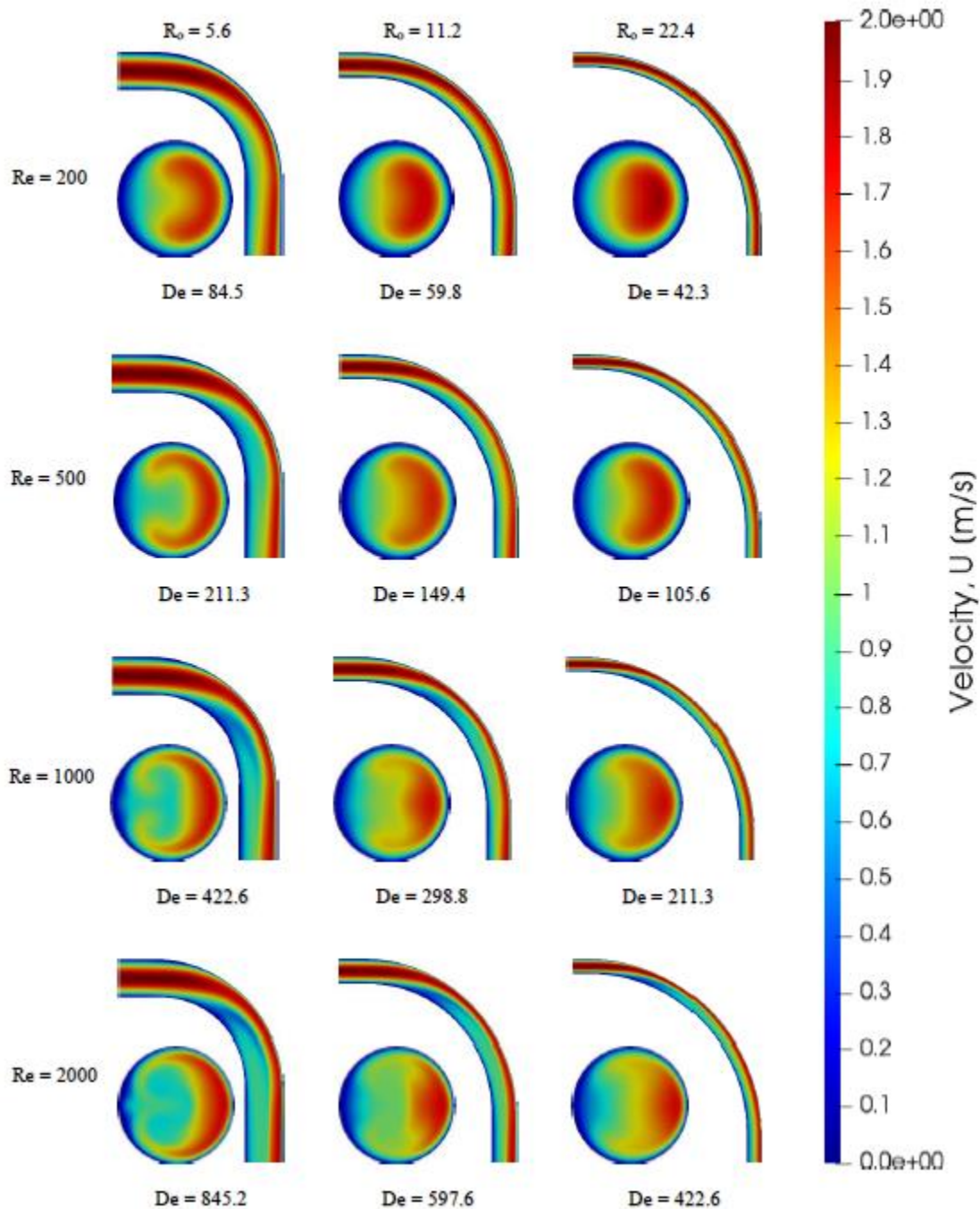show the secondary fluid flow induced by the centrifugal force.

Figure 16 Contour plots of laminar flows with different Reynolds numbers within the middle of elbows of different curvature ratios. Circular cross sections at 90-degrees (outlet of elbow) are also shown for each case

illustrates the contour plots of all combinations of Re and Ro investigated in the present study. The elbows are split along the symmetry plane (XY-plane) to reveal the contour plots in the middle. The contour shows a fully developed laminar flow within the inlet straight pipe. The flow velocity is 0 at the walls and gradually increases to a maximum value of 2m/s at the middle, which is in accordance to the expected parabolic shape. It is observed that after the flow enters

4590

the elbow part, a separation of the flow occurs due to the curvature of the elbow. The velocity region towards the inner curve of the elbow is slower relative to the region towards the outer curve. This effect results from the centrifugal force within the curved pipe. Furthermore, the flow separation is more obvious with the increasing Re by a presence of a shear layer, as shown in figure 5-7 at Re=1000 and 2000. From the elbow outlet cross sections (XZ-plane), a swirling pattern occurs. By increasing the curvature ratio, the swirling is reduced. However, when the Reynolds number increases, the swirling becomes more significant. As the Dean number increases, the swirling gets more significant. The opposite effect is observed when the Dean number decreases. Less significant swirling can be seen in the cases with lower Dean numbers compared to the cases with higher Dean numbers.

Conclusion and future work

In the present study, numerical investigations on laminar flow within elbows of varying curvature ratio has been performed. Geometric and numerical setup was performed preceding the simulations. Convergence study was conducted for multiple mesh resolutions to support selection of the optimal mesh. Mesh 2 with mesh resolution of 2321088 was evidently the optimal mesh for further study. The laminar flows investigated were in the range of 200 to 2000. Elbows with curvature ratios of 5.6, 11.2 and 22.4 were subjected to these flows of varying Reynolds number. The results from these numerical simulations provided predictions for the streamwise flow as well as the secondary flow induced by the centrifugal force of the curved pipe. The post-processed velocity contour plots illustrated how the Dean vortices of the secondary flows were generated. It was shown that the intensity of the Dean vortices increased as the Dean number increased. Furthermore, the pressure contour plots show a low-pressure region is generated towards the inner curve of the elbow, as well as a high-pressure region at the outer curve blocking the internal flow. The low-pressure region moves further downstream as the curvature ratio increases.

References

Bakker A., 2006. *Applied Computational Fluid Dynamics: Meshing.* [Online]

Cengel Y. & Cimbala J., 2017. *Fluid Mechanics.* 4th ed. Singapore: Mc Graw Hill Education.

Dean W.R. (1928). *The streamline motion of a fluid in a curved pipe*. Phil. Mag. 1. (30)

Dutta P., Saha S. K., Nandi N., Pal N. 2016. *Numerical study on flow separation in 90° pipe bend under high Reynolds number by k-ε modelling*, Engineering Science and Technology, an International Journal 19

Inthavong K. 2019. *A unifying correlation for laminar particle deposition in 90-degree pipe bends*, Powder Technology 345, Elsevier B. V.

Kim J., Yadav M., Kim, S., *Characteristics of secondary flow induced by 90-degree elbow in turbulent pipe flow*, Engineering Applications of Computational Fluid Mechanics, 8:2, 229-239, DOI: 10.1080/19942060.2014.11015509

Liestyarini, U. C., 2016. *CFD Analysis of Internal Pipe Flows*, University of Stavanger.

Nicolaou L., Zaki T. A. 2016. *Characterization of aerosol Stokes number in 90° bends and idealized extrathoracic airways,* Journal of Aerosol Science 102, Elsevier Ltd.

OpenCFD Ltd, 2016-2018. *OpenFOAM user guide*
Link: https://openfoam.com/documentation/user-guide/

Pantokratoras A. 2016. *Steady laminar flow in a 90° bend*, SAGE, DOI: 10.1177/1687814016669472

Slater J. W. 2008. *CFD Analysis Process,* NASA
Link: https://www.grc.nasa.gov/WWW/wind/valid/tutorial/process.html
Spedding P. L., Bénard E., Mcnally G. M. 2008. *Fluid flow through 90 degree bends*, Developments in Chemical Engineering and Mineral Processing, 12 (1-2). 107-128 ISSN 0969-1855, DOI: 10.1002/apj.5500120109
Sudo K., Sumida M., Hibara H. 1998. *Experimental investigation on turbulent flow in a circular-sectioned 90-degree bend*, Experiments in Fluids 25, Springer-Verlag